Evaluation of soluble benzene migration in the Uinta Basin

Y. ZHANG[1], M. PERSON[1], E. MERINO[1] AND M. SZPAKIEWCZ[2]

[1]*Department of Geological Sciences, Indiana University, Bloomington, IN, USA;* [2]*Idaho National Engineering and Environmental Laboratory, Fossil Energy Technologies, Idaho Falls, ID, USA*

ABSTRACT

Field sampling and mathematical modeling are used to study the long-distance transport and attenuation of petroleum-derived benzene in the Uinta Basin, Utah. Benzene concentration was measured from oil and oil field formation waters of the Altamont-Bluebell and Pariette Bench oil fields in the basin. It was also measured from springs located in the regional groundwater discharge areas, hydraulically down-gradient from the oil fields sampled. The average benzene concentration in oils and co-produced waters is 1946 and 4.9 ppm at the Altamont-Bluebell field and 1533 and 0.6 ppm at the Pariette Bench field, respectively. Benzene concentration is below the detection limit in all springs sampled. Mathematical models are constructed along a north–south trending transect across the basin through both fields. The models represent groundwater flow, heat transfer and advective/dispersive benzene transport in the basin, as well as benzene diffusion within the oil reservoirs. The coupled groundwater flow and heat transfer model is calibrated using available thermal and hydrologic data. We were able to reproduce the observed excess fluid pressure within the lower Green River Formation and the observed convective temperature anomalies across the northern basin. Using the computed best-fit flow and temperature, the coupled transport model simulates water washing of benzene from the oil reservoirs. Without the effect of benzene attenuation, dissolved benzene reaches the regional groundwater discharge areas in measurable concentration (>0.01 ppm); with attenuation, benzene concentration diminishes to below the detection limit within 1–4 km from the reservoirs. Attenuation also controls the amount of water washing over time. In general, models that represent benzene attenuation in the basin produce results more consistent with field observations.

Key words: benzene, Uinta Basin, water washing

Corresponding author: Ye Zhang, Department of Geological Sciences, Indiana University, 1001 East 10th Street, Bloomington, IN 47405-1405, USA.
Email: ylzhang@indiana.edu, Tel: 812-856-0139, Fax: 812-855-7899.

INTRODUCTION

In the first paper of the two-paper series (Zhang *et al.* in press), mathematical modeling is used to study soluble benzene transport and attenuation through an idealized sedimentary basin which contained an oil reservoir and an active basin-scale, topography-driven groundwater flow system. Results suggest that in basins with active groundwater flow systems, soluble benzene transport is dominated by groundwater advection and modified by bacterial degradation. The assumption that benzene transport is dominated by diffusion in the carrier bed is shown to be unlikely. These results are supported by published benzene concentration data collected at various distances from oil fields in basins across North America (Zarrella *et al.* 1967). To further test the above conclusions, a field application of the models developed in Zhang *et al.* (in press) is called for.

The Uinta Basin in northeastern Utah contains a number of well-documented oil fields (Fouch 1975), and active regional-scale groundwater flow systems (Willett & Chapman 1989; Bredehoeft *et al.* 1994). Extensive drilling has also provided high-quality geologic data that are essential for the construction of a geological framework model to compute the groundwater flow rate, temperature and solute concentration in the basin (Fouch, 1981; Pitman *et al.* 1982; Chidsey & Laine 1992; Fouch *et al.* 1992a). A topography-driven groundwater flow system extends down to depths of approximately 3 km. Oil reservoirs, such as the Altamont-Bluebell field and the Parietta Bench field contain crude oils sourced from the deeper lacustrine

source rocks of the Green River Formation. Numerous bitumen-bearing sandstone deposits are found along the southern edge of the basin (e.g. around north of Book Cliffs), indicating that biodegradation and water washing of the oils has occurred in the past. Springs and seeps can be found in the central river valleys, located in the regional groundwater discharge areas, down hydraulic gradient from the oil fields. Benzene, being the most soluble and mobile among BTEX compounds (benzene, toluene, ethylbenzne and xylene), is found in both oils and oil field formation waters in the basin. These features make the Uinta Basin an excellent natural laboratory to study the transport and attenuation of dissolved benzene in basins.

To quantify the soluble benzene transport and degradation processes in the Uinta Basin, mathematical models are constructed along a north–south trending geologic transect across the basin through both the Altamont-Bluebell field and the Parietta Bench field. This cross-sectional transect follows the general direction of the regional groundwater flow. The models represent the groundwater flow, heat transfer and advective/dispersive benzene transport in the basin as well as benzene diffusion within the oil reservoir. The coupled groundwater flow and heat transfer model is first calibrated using available hydrological and thermal data across the basin. Benzene migration in basin groundwater is then simulated with and without representing biodegradation to evaluate the impact on its transport. Field sampling of BTEX from oils and waters of the Altamont-Bluebell and Pariette Bench fields was conducted. Springs located hydraulically down-gradient from the oil fields were also sampled and analyzed for BTEX. The field measurements provide the general range of benzene concentration in oil-field formation waters to be compared with the results of the transport simulations.

In this paper, the subsurface geology and hydrology of the Uinta Basin and its oil reservoirs are first introduced. The geological transect selected for the coupled flow, heat, and transport models is described. Results of field sampling of BTEX from oil wells, oil-field formation waters, and springs are presented. We then present the results from the groundwater flow, heat-transfer and solute-transport simulations which are then summarized in the 'Discussion' and 'Conclusions' sections.

THE UINTA BASIN

Geology

The Uinta Basin is a topographic as well as a structural basin located in north-eastern Utah and north-western Colorado (Fig. 1). The basin is approximately 140 km long and 150 km wide, and is bounded by the Uinta Mountains to the north, the Wasatch Mountains to the
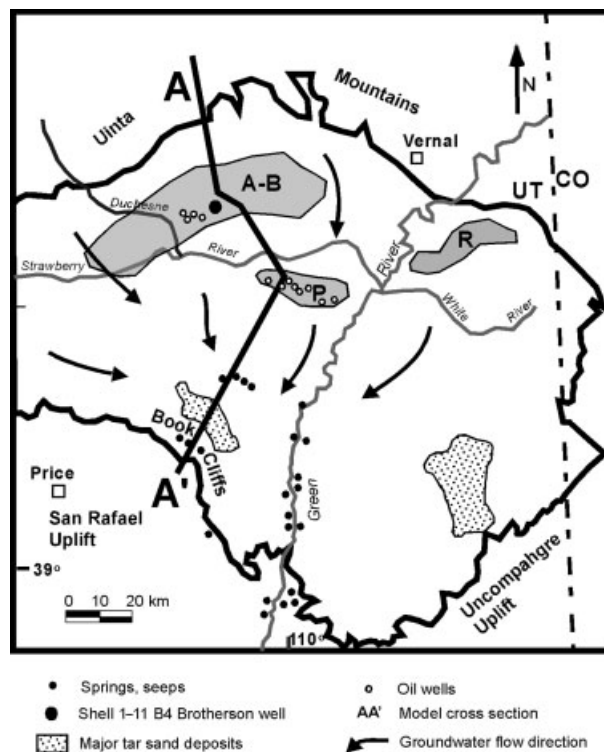
Fig. 1. The Uinta Basin along with the locations of the major oil fields (A-B, Altamont-Bluebell; R, Redwash; P, Pariette Bench), the model cross section (A–A'), and the major tar sand deposits (after Bredehoeft et al. 1994). Also shown is the location of the oil and water samples collected. The generalized directions of the regional groundwater flow are indicated by the long arrows, inferred from the potentiometric surfaces across the basin (Fig. 2).

west, the San Rafael Uplift to the south-west, the Uncomphagre Uplift to the south-east, and the Douglas Creek Arch to the east. The basin was formed during the late Cretaceous and Tertiary period with the deposition of over 3 km of sediments in a subsiding intermontane depression which hosted the ancient Lake Uinta (Bredehoeft et al. 1994). Post-depositional uplift and erosion has occurred with <1 km of Oligocene and Eocene rocks eroded (Pitman et al. 1982). Sediments in the basin consist of (i) organic-rich open-lacustrine shale and carbonate facies of the Green River Formation; (ii) marginal-lacustrine and fluvial sandstones, claystones and carbonates of the Wasatch, Colton and North Horn Formations; and (iii) fluvial and alluvial sandstones and conglomerates of the Uinta and Duchesne River Formations (Fouch 1975; Ruble & Philp 1998). Several large oil fields currently being exploited include the Altamont-Bluebell, Redwash and Pariatte Bench Fields (Fig. 1). A geochemical correlation study suggests that oil is sourced from the deeply buried open lacustrine facies of the Green River Formation (Lucas & Drexler 1975) and commonly trapped in the marginal lacustrine sandstone reservoirs of the Green

River and Wasatch Formations (Fouch 1975; Bredehoeft *et al.* 1994). As a result of extensive diagenesis, the alluvial facies is not a major reservoir unit (Fouch 1975). Excess fluid pressures are observed within the lower portion of the Green River Formation and are thought to be induced by oil generation (Bredehoeft *et al.* 1994; McPherson *et al.* 2000). Fracture porosity/permeability is critical to many productive intervals of the 'tight' Green River reservoirs (Narr & Currie 1982). Evidence from core analyses and remote sensing also suggest that microseepages of hydrocarbons may have occurred overlying the high production areas of the Altamont-Bluebell field (Lucas & Drexler 1975; Young & McCoy 1990; McCoy & Young 1992).

Groundwater hydrology

From a hydrologic perspective, three distinct groundwater flow systems exist in the Uinta Basin. Groundwater flow within the upper 2−3 km of the northern basin is characterized by normal fluid pressure in the Duchesne River Formation and the Uinta Formation (Fig. 2a). These two formations constitute one relatively permeable aquifer system. They are referred to as the Duchesne-Uinta Formations in the remainder of the text. The hydraulic head patterns in this aquifer system suggest that groundwater recharge in the basin occurs in several directions but is dominated by the flow from the north-west, driven by the topographic relief of the Uinta and Watasch Mountains. As
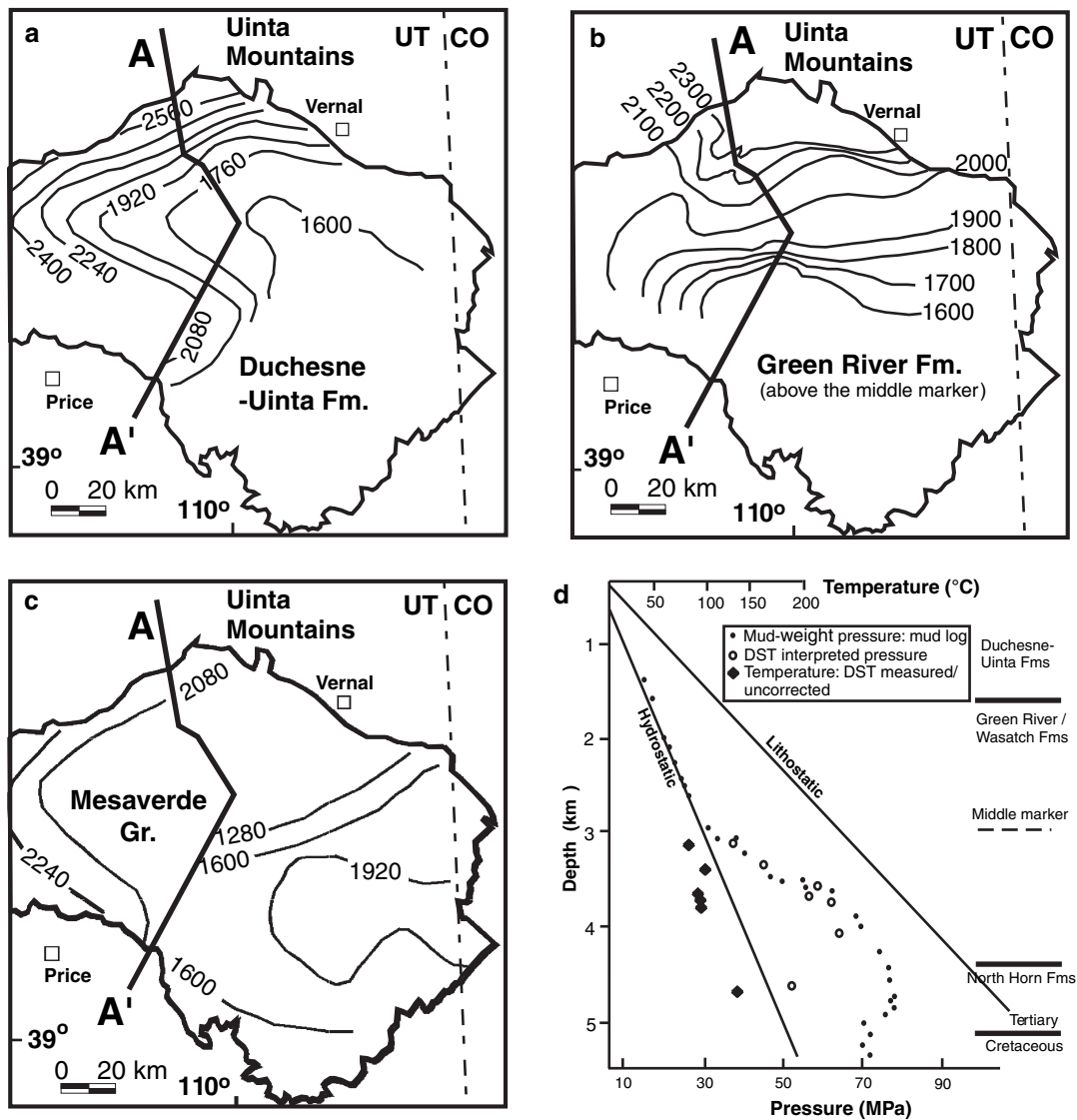
Fig. 2. The observed hydraulic head (m) in the Duchesne-Uinta Formations (a), the upper Green River Formation above the middle marker horizon (b), and the deep Mesaverde Group (c) of the Uinta Basin (after Bredehoeft *et al.* 1994; Robson & Banta 1995). Also shown are the downhole temperature and pressure measured at the Shell 1-11 B4 Brotherson well in the Altamont-Bluebell field (d) (after Spencer 1987).

a result of the higher precipitation rate and cooler surface temperature in these mountain ranges, approximately 80% of the total groundwater recharge occurs in the northern half of the basin (Utah State Water Plan − Uinta Basin 1999). The groundwater flow rates within the Duchesne-Uinta Formations are high enough to disturb the subsurface conductive temperature field (Fig. 3). Negative thermal anomalies in excess of 20°C have been observed adjacent to the Uinta Mountains, corresponding to the regional groundwater recharge areas (Willett & Chapman 1987, 1989). Positive thermal anomalies have also been observed along the southern portion of the B-B′ transect near the central river valley (Fig. 3), corresponding to the regional groundwater discharge areas. Vitrinite reflectance data also suggest that the present thermal anomalies may have existed during much of the basin history (Willett & Chapman 1987), indicating that the present groundwater flow systems in the basin may have existed for millions of years.

In the northern half of the basin, the Duchesne-Uinta formations overly the Green River Formation, the Wasatch Formation, and the upper Cretaceous undifferentiated Mesaverde Group. Groundwater within the upper Green River Formation (above the middle marker horizon) has normal fluid pressure, and is driven by the water-table gradient of the Uinta Mountains (Fig. 2b). In the lower Green River Formation below the middle marker, formation fluids in the Altamont-Bluebell field are significantly over-pressured at depths between 3000 and 5000 m (Fig. 2d) (Spencer 1987). The 5418-m-deep Shell 1-11 B4 well is considered representative of the geology and pressure conditions of the Altamont-Bluebell field (Bredehoeft et al. 1994). In parts of this field, fluid pressure reach 80%
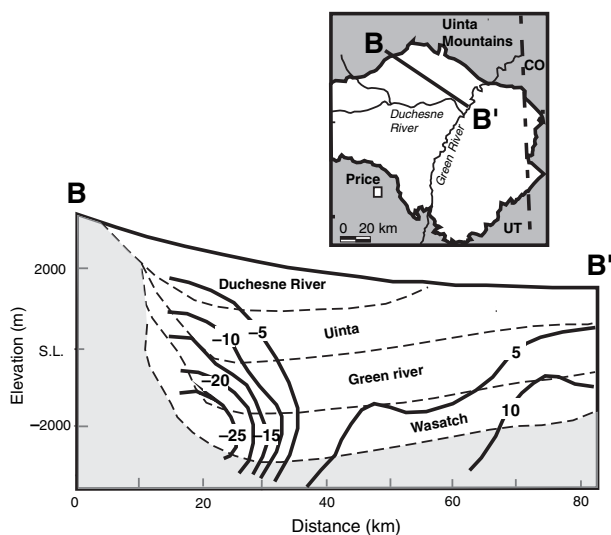
of lithostatic pressure (Fig. 2d). Such excess pressure is thought to be caused by hydrocarbon generation and is also believed to affect the regional groundwater flow patterns at depths (Sweeney et al. 1987; Bredehoeft et al. 1994; McPherson & Bredehoeft 2001). The mechanism of over-pressure generation by sediment loading appears unlikely because the Uinta Basin is now undergoing erosion. However, it is possible that fossil over-pressure from past loading events could have remained in the basin, e.g. the rapid deposition of 3-km-thick Green River clay. To estimate a relaxation time for this compaction-driven over-pressure, a response time equation can be used:

$$\tau = \frac{S_s L^2}{K} \tag{1}$$

where τ is the relaxation time, L, S_s and K are the thickness, specific storage, and hydraulic conductivity of the low-permeability deposits, respectively. Using typical values for clayey sediments ($S_s = 10^{-3}$ m^{-1}; K_{clay}: 10^{-8}–10^{-11} m sec^{-1}; Freeze & Cherry 1979), a relaxation time is estimated to range from 0.03 to 28 million years for the deposition of approximately 3 km of the Green River clay. This relaxation time is less than the time since the Green River deposits ceased deposition, as the younger, more permeable Duchesne River Formation ceased deposition at 32 Ma (McPherson & Bredehoeft 2001). Thus it appears unlikely that the current over-pressure is the remnant of past sediment-loading.

Underlying the over-pressured lower Green River Formation, within the rocks of the Mesaverde Group, fluid pressure drops to sub-hydrostatic levels (Fig. 2c), suggesting that these rocks act as a drain for the overlying formations. In summary, an upper normal-pressured flow system exists in the Uinta Basin within the relatively permeable Duchesne-Uinta Formations. This flow system is underlain by the mainly low-permeability Green River Formation which can be further divided into an upper normal-pressured zone and a lower over-pressured zone. A basal Mesaverde Group lies beneath the Green River Formation with fluid pressure below normal.

Lithostratigraphy

The cross-sectional model developed for this study is based on the geologic data presented by Fouch (1975), Pitman et al. (1982), and Bredehoeft et al. (1994) (Fig. 4). The cross-section extends from the Uinta Mountains in the north to the south of the Books Cliff, crossing both the Altamont-Bluebell field and the Pariette Bench field (Fig. 1). It has a total length of 142 km and a maximum thickness of 8.8 km. It consists of 18 lithostratigraphic units (note that the Duchesne River Formation and the Uinta Formation are represented separately). The major stratigraphies represented by the cross section include the

Fig. 3. A contour map of the estimated temperature anomalies (in °C) in the northern Uinta Basin along transect B−B′, reported as deviations from a conductive temperature field (after Willett & Chapman 1989).
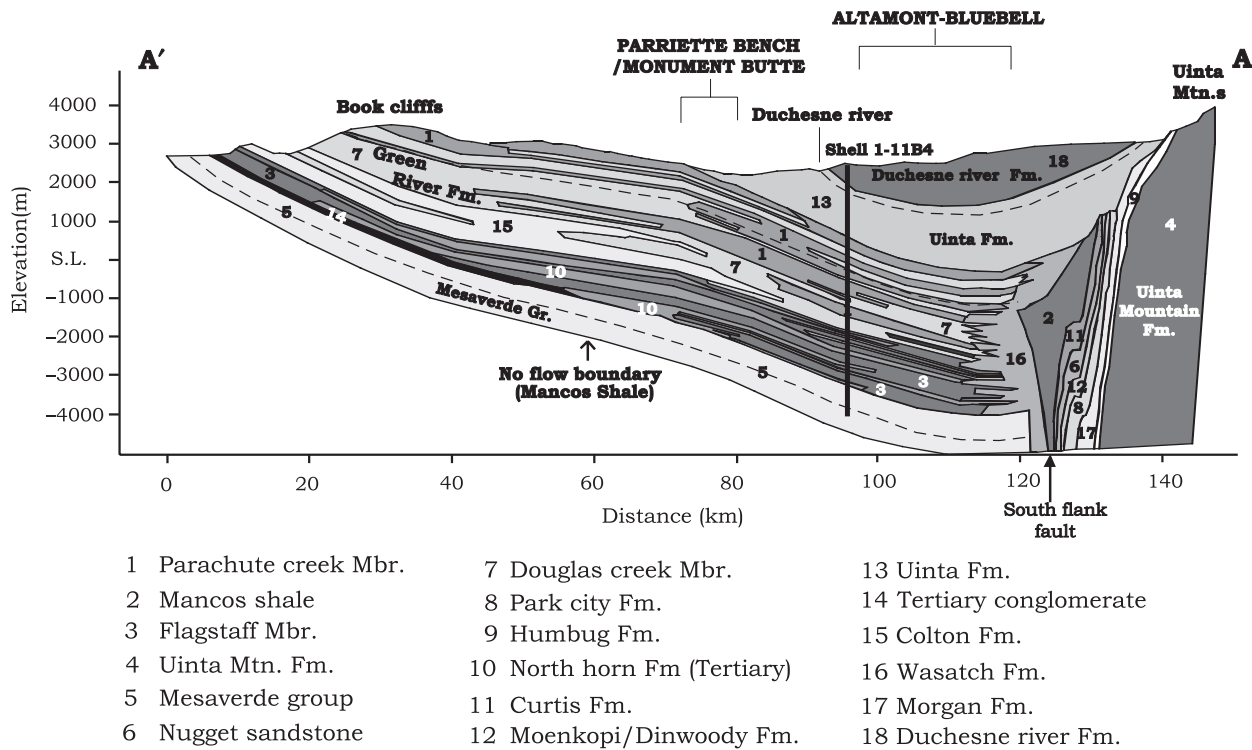
Fig. 4. The 18 lithostratigraphic units represented by the cross-sectional transect A-A′ (after Fouch 1975; Pitman *et al.* 1982; Bredehoeft *et al.* 1994). The locations of the Uinta Mountains, Book Cliffs, Duchesne River and the Shell 1-11 B4 well are indicated, as well as the Altamont-Bluebell and Pariette Bench oil fields. Three dashed lines indicate the depths at which the computed head is calibrated against the observed head (Fig. 9).

Mesaverde Group, the North Horn Formation, the Colton Formation, the Wasatch Formation, the Green River Formation, the Duchesne-Uinta Formations, and the Uinta Mountain Formation. Thin layers of Paleozoic and Mesozoic rocks are thrust upwards along the South Flank Fault between the Wasatch Formation and the Uinta Mountain Formation. These rocks are, in general, permeable formations. The Green River Formation is further subdivided based on the lithofacies types. Notably, the Flagstaff Member is an open lacustrine carbonate-and-shale source rock, and the Douglas Creek Member is composed of marginal lacustrine sandstones which serve as hydrocarbon reservoirs in some oil fields. In the Altamont-Bluebell field, the Flagstaff source rock is interbedded with the North Horn Formation. In the southern portion of the basin, the Parachute Creek Member and the Douglas Creek Member of the Green River Formation form extensive outcrops, along with the Tertiary deposits of the North Horn Formation, Colton Formation and thin layers of the Green River conglomerates. Below the Mesaverde Group is the Mancos shale (which is assumed, in this study, to constitute an impermeable base to our model). Overall, the cross-sectional transect follows the general direction of regional groundwater flow in the basin and is used to construct a two-dimensional geological framework model of the basin.

Oil reservoirs

Most of the hydrocarbon production within the Uinta Basin is from the over-pressured Altamont-Bluebell oil field within the Green River Formation in north-western Uinta Basin (Fig. 1). Crude oil produced from this field is paraffinic, being derived from type I kerogen (Ruble *et al.* 2001). The producing intervals of this field are located at a depth range of 2400−5200 m, generally coinciding with the over-pressured zone. The open lacustrine facies of the Flagstaff Member within the lower Green River Formation serves as the oil kitchen and the inter-bedded layers of marginal lacustrine sandstones serve as reservoir units (Lucas & Drexler 1975). Most of the oil is hosted in a thick section (760−915 m) of fractured, low-porosity sandstones, shales, and carbonates (Spencer 1987). The Altamont-Bluebell field is not a classical example of an oil reservoir as its source rock, reservoir unit, or cap rock cannot be clearly differentiated. Oil generation and reservoir charging occurs even now despite the cooling trend associated with the erosion in the basin. Based on the bottom-hole temperature measurements, fluid temperature within the Altamont-Bluebell field ranges from 80 to 130°C (Fig. 5). The scatter of the data shown in this figure is possibly due to the variations in the geothermal gradient across the basin. The average geothermal gradient for the
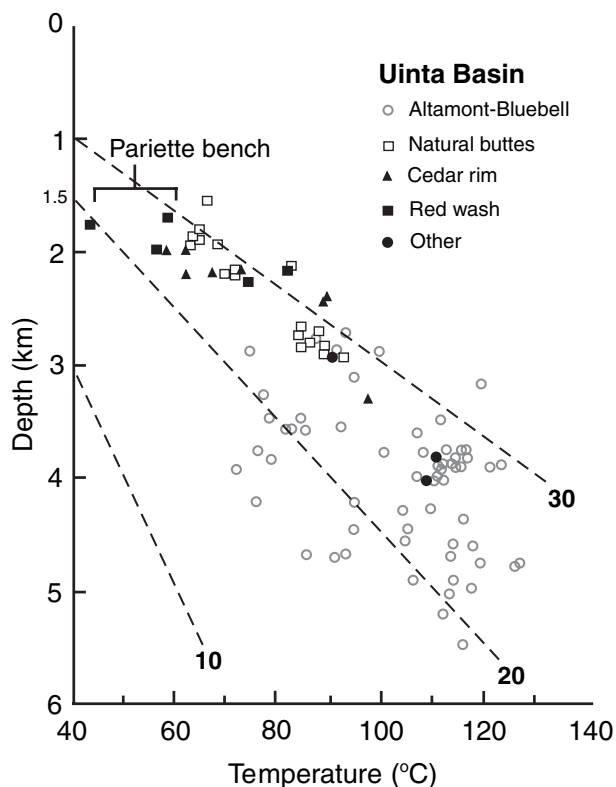
Fig. 5. Bottom-hole temperature (°C) versus depth from different hydrocarbon-producing fields in the Uinta Basin (after Chapman *et al.* 1983). Three geothermal gradients (dashed line in°C km^{-1}) are plotted assuming a surface temperature of 10°C.

Uinta Basin is estimated to be 25°C km^{-1} (Chapman *et al.* 1983).

The Pariette Bench oil field lies to the south-east of the Altamont-Bluebell field (Fig. 1). Oil produced from this field is hosted in fractured, low-porosity, marginal lacustrine sandstone facies of the Douglas Creek Member of the Green River Formation (Pitman *et al.* 1982). The reservoir lies at a depth of approximately 1500 m. The source rocks present in the Pariette Bench field are thermally immature and the oil of this field is generally believed to have migrated into this reservoir from the deeper Green River source rocks (Pitman *et al.* 1982). The Pariette Bench field has normal fluid pressure (Pitman *et al.* 1982) and an inferred bottom-hole temperature range of 45–60°C (Fig. 5). Given the moderate observed temperature range, biodegradation of benzene may have occurred in this field.

FIELD SAMPLING IN THE UINTA BASIN

A total of 17 samples of oils and co-produced formation waters were collected from production wells completed in the Green River Formation in the Uinta Basin between October 1999 and March 2000 (sample locations shown in Fig. 1). Pariette Bench oil wells were sampled first in

October 1999. In March 2000, oil/water samples were collected from four deep wells completed in the Altamont-Bluebell field. In the oil fields, borehole samples were taken from the wellheads whenever possible. Note that because of the volatility of BTEX, their concentration in the wellhead samples may be biased towards lower values than the *in situ* concentration at the reservoir temperature and pressure conditions. In the meantime, a search for perennial springs and seeps was carried out within the discharge areas of the basin. The springs of enhanced temperature and mineralization were selected, indicating regional flow origin. A total of 22 springs are identified, ranging from several kilometers to tens of kilometers hydraulically down-gradient from the oil fields sampled. As BTEX are volatile, the oil and water samples were collected from their sources into tightly capped glass containers as quickly as possible. In general, we tried to maintain a minimum contact of the samples with the atmosphere during sampling. To prevent further loss of these dissolved aromatics from solutions, the water samples were not filtered or acidified.

Analytical procedure

All samples collected are analyzed for BTEX in the Idaho National Environmental and Engineering Laboratory (INEEL) using gas chromatography (GC) with a purge and trap extraction method. Samples are analyzed using a Stabilwax−DA [30 m × 0.25 mm internal diameter × 25 μm df] column in a HP 5890 Series II GC. The initial temperature is set at 30°C for 2 min, ramping at 5°C min^{-1} to 75°C, ramping again at 20°C min^{-1} to 100°C and held for 2 min. The carrier gas is helium with 15 psi dictating the flow rate, the injector is at 150°C and the detector is a flame ionization detector (FID) at 175°C. Samples are transferred into a glass tube and connected to the OIAnalytical 4560 Purge and Trap system. The purge temperature is 30°C for 3 min, the desorb temperature is 240°C for 4 min, and the temperature is 240°C for 10 min. The valve and the transfer line temperature are set at 200 and 150°C, respectively. The GC analyses take 14.25 min each and the purge and trap is 22 min. A four-point calibration is used with the standards bracketing the possible concentration of the samples. The calibration standards are prepared in the laboratory. The certified calibration standards (2%) from AccuStandard Inc. are used to check quality control. For all samples, the BTEX detection limit is set to 10 ppb, or approximately 0.01 ppm.

Sampling results

BTEX concentration measured from the oil wells in the Uinta Basin are grouped into two categories: those from the deep, over-pressured Altamont-Bluebell field and those from the shallower, normal-pressured Pariette Bench field

Table 1 (A) BTEX concentration (ppm) measured from oils and oil field formation waters of the Pariette Bench and Altamont-Bluebell fields, Uinta Basin, Utah. (B) Benzene concentration measured from oil field formation waters in different basins across North America is listed (after Zarrella *et al.* 1967; Burtell & Jones 1996).

(A)

Location	Benzene[*1] C_{oil}	C_{aq}	C_{oil}/C_{aq}	Toluene (C_{aq})	Ethylbenzene (C_{aq})	o, m, p-Xylene (C_{aq})
Pariette Bench						
Hendle #1	–	0.45	–	0.42	0.03	0.05
Eight Mile Flat – Balcron Fd.	–	0.13	–	0.16	0.02	0.04
Eight Mile Flat - # 32-29-T	–	0.21	–	0.36	0.02	0.04
S. Pleasant Valley # 2-22-g-17	1412.7	0.57	2478	0.61	0.05	0.07
S. Pleasant Valley # 41-30-H	981.5	0.42	2337	0.26	3.26	0.40
Castle Peak Fd. # 6-23	–	0.02	–	ND	ND	0.07
Castle Peak Fd. # 32-1-J	–	0.30	–	0.04	ND	0.05
Castle Peak Fd. # 43-10-g-16	–	0.49	–	0.84	0.06	0.12
Outside Castle Peak area # 31-21-g-16	–	0.39	–	0.67	0.04	0.09
Outside Castle Peak area # 31-20-G	–	0.50	–	0.67	0.04	0.09
Ashley Wells # 10-23-g-15	1533.1	0.63	2433	0.83	0.07	0.15
Monument Butte # 2-35-8-15	2207.8	1.03	2143	1.43	0.11	0.31
Monument Butte # 2-35-8-15 (well head)	865.1	0.88	983	1.03	0.06	0.15
Altamont-Bluebell						
Chasel Sprouce # 1-18	19298.5	3.76	5133			
Wade Cook # 2-14 AI	2237.9	9.48	236			
Bowen Bastian # 1-14	722.0	3.31	218			
Sasha 4-6-A2 (Tribal well)	1655.2	5.95	278			

(B)

Field	Location	Geological Formation	Concentration (mg l^{-1})
Formation waters co-produced with oil			
Bough	Lea Co., N.M.	Pennsylvanian	10.7
Golden Spike	Alberta	Basal Quartz	7.1
Lampman	Saskatchewan	Frobisher-Alida	7.0
Keystone	Crane Co, Tex.	Holt	4.7–5.6
Stettler	Alberta	Leduc	4.8–6.0
Stettler	Alberta	Nisku	4.9–6.0
Darst Creek	Texas	Edwards Is	0.21
Geological Formation			
Formation waters at a distance to production			
Rundle Fm. in Alberta, Canada			0.1
Paradox Fm. in New Mexico			0.15–2.7
Sligo Fm. in Mississippi			0.25–6.5

[*1] Only benzene was measured from oils and formation waters of both fields.
C_{oil} is the concentration in oil; C_{aq} is the concentration in oil-field waters.

(Table 1A). Among BTEX, only benzene concentration is measured from both oil and oil-field formation waters. The median benzene concentration in oils and co-produced formation waters is 1946 and 4.9 ppm at the Altamont-Bluebell field and 1533 and 0.6 ppm at the Pariette Bench field, respectively. At the Pariette Bench field, eight formation water samples are collected from wellheads with no oil. Benzene concentration in these waters ranges from 0.02 to 0.5 ppm, generally lower than its concentration found in waters co-produced with oils in the same field (0.4–1.0 ppm). Benzene concentration measured in oil-field formation waters from other basins across North America is also listed (Table 1B). Formation water samples in these basins have been collected from both production wells and test wells. Similar to the Pariette Bench field, benzene concentration tends to be higher in formation waters co-produced with oil and lower if sampling was conducted a distance away from the producing zones. Overall, benzene concentration in oils is approximately 2 to 3 orders of magnitude higher than that in formation waters. The variations of benzene concentration measured in oils from the same field are probably because of the heterogeneity in oil composition or differential loss during production/sampling. The variations of benzene concentration in formation waters from the same field are probably because of the heterogeneity of the oil composition in

contact with the waters, the temperature variations in the sampled formation intervals, or miscible transport by groundwater (as higher benzene concentration is often found in co-produced waters than in formation waters sampled from non-producing intervals/wells).

With the exception of the Chasel Sprouce #1-18 and Monument Butte #2-35-8-15 wells, the ratios of benzene concentration in oils and co-produced waters display remarkable constancy for each field (Table 1A), suggesting equilibrium partition of benzene between oils and formation waters. The differences in the ratio C_{oil}/C_{aq} between the two fields are probably because of the effects of temperature on the equilibrium partition coefficient. The hotter Altamont-Bluebell field has a higher partition coefficient (see Fig. 6 in Zhang *et al.* in press), and thus a higher ratio of benzene concentration in water relative to oil. Benzene concentration measured from *spring* water samples collected in the basin is below the detection limit. This suggests that benzene migrating away from these two oil fields does not reach the down-gradient discharge areas because of possible attenuation along the transport path.

Note that the oil/water sampling conducted in this study serves to indicate the magnitudes of benzene concentration in oils and oil field formation waters in the Uinta Basin. These values are consistent with the benzene concentration measured in other oil-producing basins. Although the collection or measurement methods may introduce biases and uncertainties, the above general observations are probably valid. Note also that for both oil reservoirs modeled, our goal is to identify the end-member

scenarios that can impact benzene migration (no attenuation versus attenuation with an upper limit of biodegradation rate constant). The computed concentration is not conditioned by the measured values. Rather, the measurements provide us with a general range of values to compare with the model results to aid in the final discussions on the coupled benzene transport process in the Uinta Basin.

MODEL APPLICATION

Model description

To simulate soluble benzene transport in the Uinta Basin, hydraulic head, groundwater flow rate and temperature in the basin are first calculated. The simulated head and temperature are compared with the observed pressure and temperature conditions across the basin. Using a best-fit flow and temperature field, the transport and attenuation of benzene in groundwater and its diffusion within the oil reservoirs are then simulated. A detailed description of the mathematical models can be found in Zhang *et al.* in press. To model the groundwater flow in the Uinta Basin, a fluid-source term is added to the right-hand side of the flow equation (Equation (1); Zhang *et al.* in press) to represent the excess head in the lower Green River Formation:

$$\nabla \cdot [\rho_f \mu_r \mathbf{K} \nabla(h + \rho_r z)] = \rho_{oil} q' \qquad (2)$$

where ρ_{oil} is the oil density, q' is the oil generation source strength (year^{-1}), all other symbols are defined in Equation
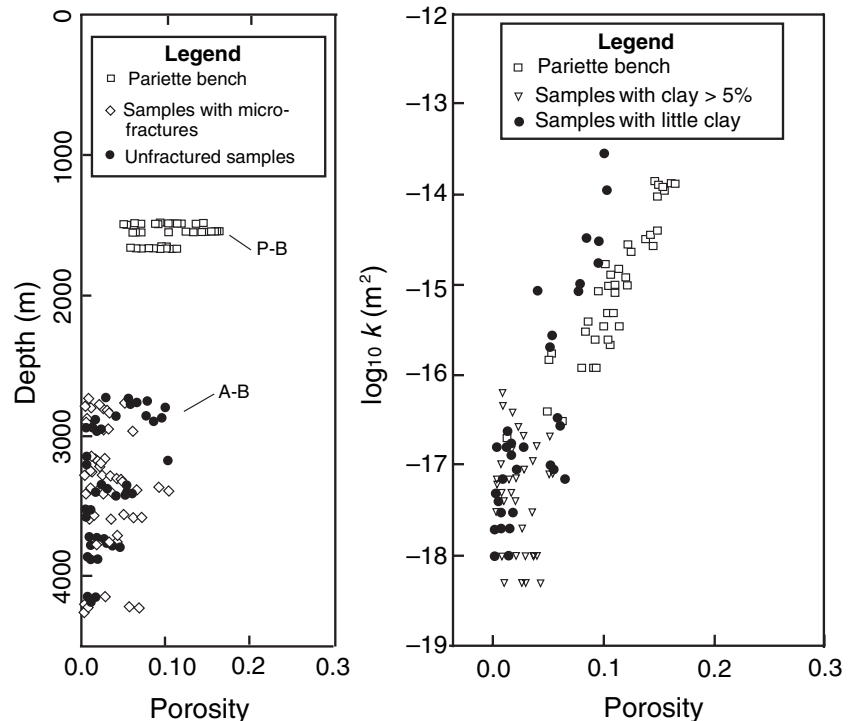
Fig. 6. Porosity-depth and porosity-permeability measurements from rock samples in the Uinta Basin (after Pitman *et al.* 1982; McPherson & Bredehoeft 2001). Besides the core data of the Pariette Bench field (P-B) (Pitman *et al.* 1982), all other data came from core plug measurements of the Green River Formation in the Altamont-Bluebell field (A-B).

(1) in Zhang et al. (in press). q' represents oil generation to create excess pressure as the volume of kerogen consumed is less than that of oil generated, and hence oil generation acts as a fluid-source term. This approach is similar to that used by Bredehoeft et al. (1994) and McPherson et al. (2000) to represent over-pressure in the lower Green River Formation. The above equation is also capable of representing groundwater flow induced by water table topography and fluid-density variation.

Permeability and porosity for each lithostratigraphic unit are assigned based on available published data on Uinta Basin rocks (Fouch 1975; Pitman et al. 1982; Fouch et al. 1992b; Schmoker et al. 1992; Hester & Schmoker 1993; Bredehoeft et al. 1994; McPherson & Bredehoeft 2001) (Table 2). The permeability and porosity are estimated with a variety of methods including core-plug measurements, drill-stem tests, porosity-depth inference, or numerical modeling. Shown in Fig. 6 are some of the core measurements of porosity/permeability on rocks of the Altamont-Bluebell field (McPherson & Bredehoeft 2001) and the Pariette Bench field (Pitman et al. 1982). The permeability measurements of the Altamont-Bluebell field are from unfractured samples only. Clearly, in the Uinta Basin, porosity and permeability decrease with increasing depth. At the Altamont-Bluebell field at depths >3000 m, porosity is generally <10%, and the corresponding permeability is <10^{-16} m^2. At the Pariette Bench field (at depths

approximately 1500 m), permeability is higher, ranging from 10^{-14} to 10^{-16} m^2. As part of a model calibration exercise to compute the groundwater flow rate and temperature in the basin, permeability of the upper Duchesne-Uinta Formations, the Douglas Creek Member of the Green River Formation, and the basal aquifers of the Mesaverde Group is varied within its range of uncertainty (indicated in Table 2). For the heat-transfer simulation, a fluid phase thermal conductivity of 0.59 W m^{-1} K^{-1} and heat capacity of 4.18E + 3 J kg^{-1} K^{-1} are used. Depending on the lithofacies type, the thermal conductivity of the solid phase varied between 2.0 and 3.1 W m^{-1} K^{-1} (Garven 1989). A longitudinal and transverse dispersivity of 100.0 and 10.0 m are assigned for the heat transfer and solute transport models, respectively. These values fall within the observed range typically estimated for kilometer-scale groundwater flow systems (Gelhar 1993).

To create a geological framework model of the basin for the simulations, the cross-sectional lithostratigraphy presented in Fig. 4 is discretized with 14 544 nodes and 28 768 triangular elements using the Argus^{TM} mesh generation package. Depending on the bed thickness, the size of the triangle elements varies between 50 and 500 m. The Altamont-Bluebell oil reservoir and the Pariatte Bench oil reservoir are represented in separate simulations (Fig. 7). The location and size of the Altmont-Bluebell reservoir is determined from the known production depth intervals as well as the general range of the over-pressured zone indicated by Fouch (1975). The grid for the Altmont-Bluebell reservoir consists of 767 nodes and 1404 elements, while that of the Pariatte Bench reservoir consists of 76 nodes and 118 elements.

For the groundwater flow and temperature simulation, a specified head equal to the water table elevation of the basin is assigned to the top boundary of the model basin (Tóth 1963). No-flow conditions are imposed on the side and the bottom of the basin. A specified temperature of 10°C is assigned to the top boundary and a constant heat flux of 60 mW m^{-2} is assigned at the base. These values represent the average surface temperature as well as heat-flow conditions across the basin (Chapman et al. 1983). Because the side of the Uinta Basin model at the Uinta Mountain Formation is sub-vertical, a heat flux boundary is also assigned to it with the magnitude of the heat flux proportional to its slope (Mailloux et al. 1999). For the solute-transport simulation, the initial benzene concentration is assigned to be 0.0 ppm everywhere across the basin (outside the oil reservoir). The side and the bottom of the basin are no-flux boundaries, while a constant zero concentration is assigned to the top boundary except along the areas of groundwater outflow where a discharge boundary condition is specified ($\partial C/\partial z = 0.0$). An internal mass in-flux boundary is assigned at the oil−water contact. Accordingly, an out-flux boundary is assigned to the diffusion

Table 2 Lithostratigraphic units corresponding to Fig. 4 and the associated log-permeability and porosity values assigned to the Uinta Basin groundwater flow model.

Unit	Formation	Member	Log Permeability (m^2)	Porosity
1	Green River	Parachute Creek	−17.7	0.037
2	Mancos Shale		−19	0.23
3	Green River	Flagstaff	−17.4	0.003
4	Uinta Mts.		−18	0.1
5	Mesaverde Group*		−15 to −17	0.09
6	Nugget Sandstone		−16	0.065
7	Green River*	Douglas Creek	−15 to −17	0.1
8	Park City		−16	0.028
9	Humbug		−14	0.15
10	North Horn		−17	0.093
11	Curtis		−16	0.13
12	Moenkopi Dinwoody		−18	0.35
13	Uinta*		−13 to −15	0.15
14	Green River	Tertiary Conglomerate	−15	0.096
15	Colton		−16	0.115
16	Wasatch		−17	0.13
17	Morgan		−13	0.2
18	Duchesne River*		−13 to −15	0.2

Formation indicated with an asterisk includes a range of permeability; permeability of the formation is varied within this range as part of a model calibration exercise.
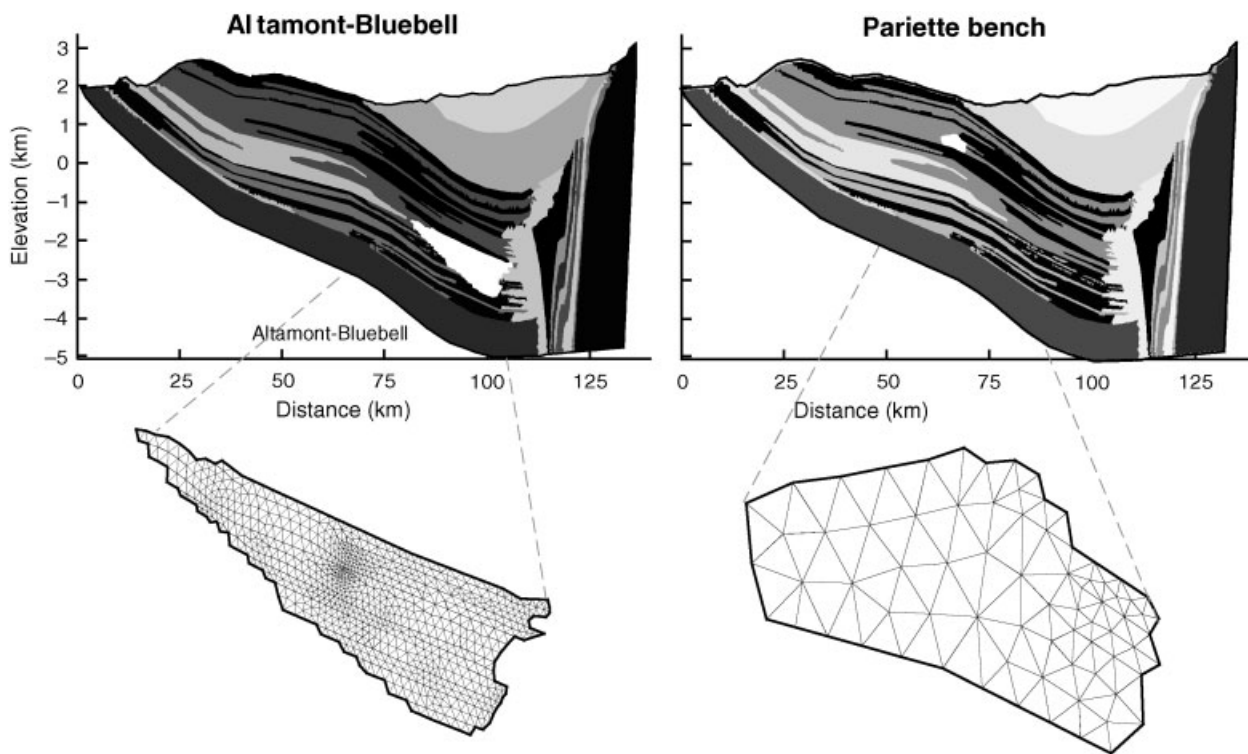
Fig. 7. The lithostratigraphic transect across the Uinta Basin along with the location of the modeled oil reservoirs. The finite element grids used to represent the oil reservoirs are also shown.

model representing the oil reservoir. The initial benzene concentration in the oil reservoir is uniformly assigned to be 1946 ppm in the Altamont-Bluebell reservoir and 1533 ppm in the Pariette Bench reservoir, corresponding to the medium values measured in these fields.

Model calibration

In the groundwater flow and heat transfer simulation, permeability of the Mesaverde Group, the Douglas Creek Member of the Green River Formation, and the Duchesne-Uinta Formations is adjusted within its range of uncertainty. The oil generation strength [q' in Equation (2)] of the Flagstaff source rock is also varied to simulate the high fluid pressure at the lower Green River Formation. The temperature anomalies are computed by taking the difference between the simulated temperature and an equivalent conductive temperature field. In the model calibration exercise, numerous model simulations are conducted to produce results consistent with the observed head (Fig. 2a, b, c), the observed downhole pressure and temperature at the Altamont-Bluebell field (Fig. 2d), and the observed thermal anomalies across the northern basin (Fig. 3). Best-fit agreement is reached when the Douglas Creek Member of the Green River Formation is assigned with a relatively low permeability ($10^{-17.3}$ m^2), and both

the upper Duchesne-Uinta Formations and the basal Mesaverde Group are represented as relatively permeable units ($10^{-14.7}$ m^2 for the former and $10^{-15.3}$ m^2 for the latter). To simulate the excess head observed in the Altamont-Bluebell field, an oil-generation source term of 17.5 year^{-1} is found via calibration. In general, the calibrated permeabilities are consistent with the results from earlier modeling studies of Willett & Chapman (1989), Bredehoeft et al. (1994), and McPherson & Bredehoeft (2001). The best-fit permeability of the Douglas Creek Member is lower than the range (10^{-14}–10^{-16} m^2) of permeability measured on core samples of the Pariette Bench field (Fig. 6). However, these permeability measurements were taken at the surface temperature and pressure conditions; the *in situ* permeability is expected to be much lower (Pitman et al. 1982). For example, Keighin & Sampath (1980) reported as much as 80% reduction in permeability, when sandstones of the Uinta Basin were subject to pressure conditions approximating subsurface reservoirs.

The best-fit, computed hydraulic head and groundwater flow rate across the basin indicate that three distinct groundwater flow systems exist in the basin. The upper flow system consists of the upper Uinta Mountain Formation and the aquifers of the Duchesne-Uinta Formations in the northern half of the basin (Fig. 8a). Groundwater flow within these formations is driven by the high water table
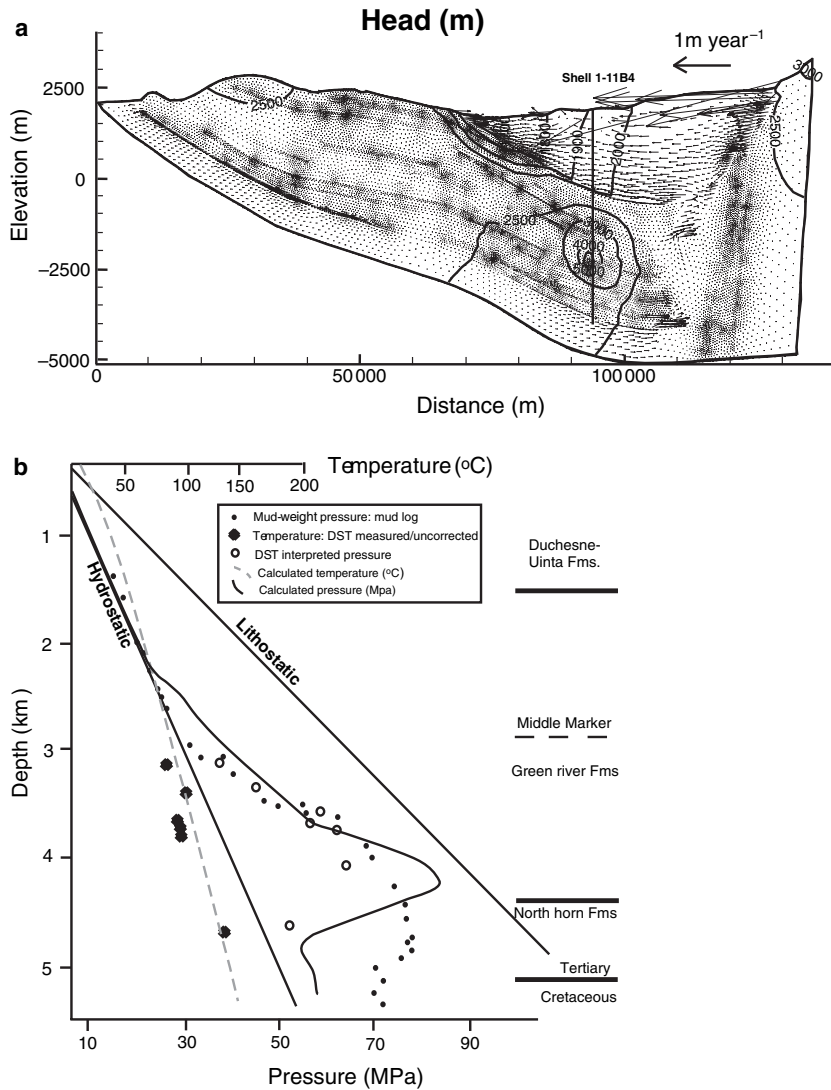
Fig. 8. (a) The best-fit hydraulic head (m) and groundwater velocities (m year^{-1}) computed for the Uinta Basin. Location of the Shell 1-11 B4 well is indicated by a bold line. (b) The best-fit, computed down-hole temperature and pressure along this well, compared with the observed temperature and pressure.

elevation of the Uinta Mountains. Compared with the more deeply buried formations within the model basin, this dominantly gravity-driven groundwater flow is the most vigorous with an average horizontal flow rate of 0.2 m year^{-1}. The best-fit computed head profiles along the Duchesne-Uinta Formations are consistent with the observed head (Fig. 9a). Beneath this shallow flow system, groundwater within the low-permeability (10^{-17}–10^{-18} m^2) Green River and North Horn Formations is characterized by much lower flow rate (on the order of 10^{-4} m year^{-1}) (Fig. 8a). As a result of the fluid-source term introduced to represent oil generation within the Flagstaff source rock, groundwater in the lower Green River Formation at the Altamont-Bluebell field is over-pressured (see the closed head contours intersected by the Shell 1-11 B4 well). The maximum computed head reaches 3000 m above the hydrostatic level. This over-pressured zone significantly impacts the groundwater flow patterns at

depth; groundwater is driven outward away from the center of the highest head. Some of the groundwater flows northward into the Wasatch Formations near the South Flank Fault where it mixes with the descending meteoric water coming through this fluid conduit. As a result, groundwater flow patterns in this region are affected by both the high head of the Uinta Mountains to the north and the high head of the Altamont-Bluebell field to the south. The best-fit computed temperature and pressure profiles in the Altamont-Bluebell field are also consistent with the observed values at the Shell 1-11 B4 well (Fig. 8b). The depth of the simulated over-pressure ranges from 2.3 to 5 km, slightly higher than the observed interval. The shape of the computed pressure profile is also less diffused compared with the observed profile. This is probably because a uniform oil generation term is assumed for the Flagstaff source rock over varying temperature (the temperature range for the entire Altamont-Bluebell field is
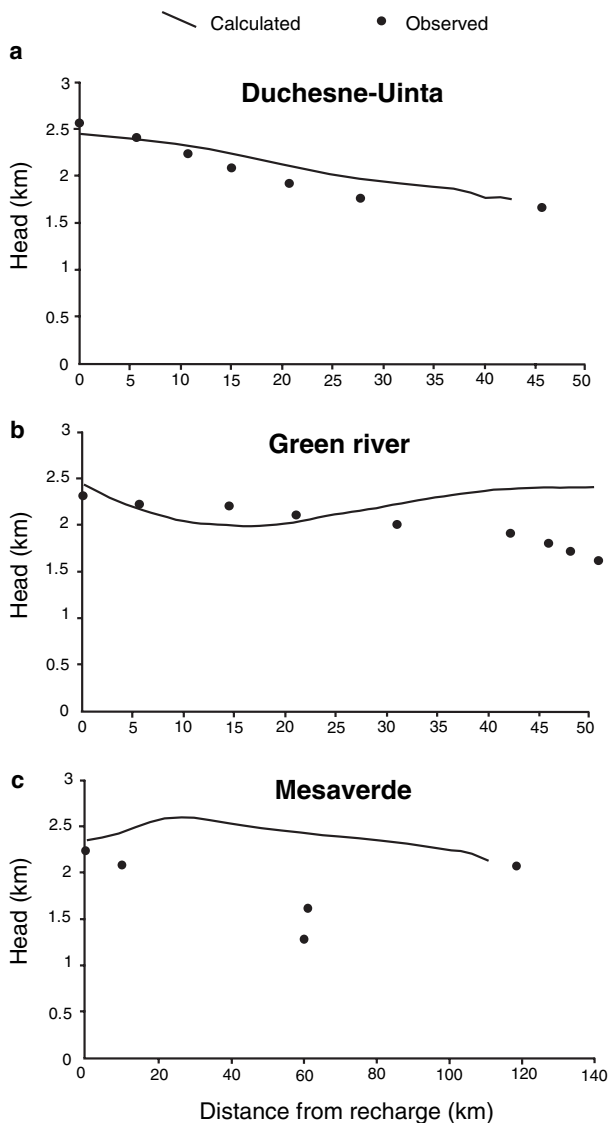
Fig. 9. The computed hydraulic head (km) versus distance from recharge in the Uinta Basin in (a) the Duchesne-Uinta Formations, (b) the upper Green River Formation (above the middle marker), and (c) the basal Mesaverde Group. The observed head is also shown (dots). The computed head is sampled along the dashed lines shown in Fig. 4; the observed head comes from the potentiometric maps shown in Fig. 2.

The computed head profile along the length of this group is further representative of many confined aquifer systems (Fig. 9c). However, the observed head near the central basin is significantly under-pressured, possibly due to the existence of a larger-scale regional flow system extending into the underlying formations that is not represented by the cross-sectional model. The Mancos shale (the impermeable base assumed for the model) may be fractured, connecting groundwater in the basal Mesaverde Group with the flow systems from the nearby Paradox basin to the south-east. Because the Paradox basin lies at a lower elevation than the Uinta Basin, such a connection would inevitably reduce the fluid pressure within the Mesaverde Group.

The overall computed groundwater flow patterns in the basin suggest that most of the recharge occurs in the Uinta Mountains to the north where the water table is the highest. Most of the groundwater discharges into the central river valleys, issuing water from both the upper Duchesne-Uinta aquifers and the deeper Green River Formation. Some of the recharge from the Uinta Mountains descends downward through the fluid conduit of the Wasatch Formation and older rocks near the Southern Flank Fault, before mixing with the groundwater flowing north from the Altamont-Bluefell field. In addition, the high groundwater flow rate in the upper Duchesne-Uinta aquifers has caused significant temperature deviations from a conductive geothermal field (Fig. 10). This is consistent with the observed temperature anomalies in the northern half of the basin (Fig. 3). However, in the southern portion of the basin, where the Green River Formation outcrops, the temperature field is mainly conductive. The computed, best-fit temperature in the Altamont Bluebell field ranges from 90 to 150°C, slightly higher than the observed range. The computed temperature for the Pariette Bench field ranges from 40 to 50°C, generally falling within the range inferred from the bottom-hole temperature measurements (Fig. 5).

The best-fit, computed head and temperature are considered a reasonable representation of the observed pressure/temperature conditions in the Uinta Basin. The resulting flow field is believed to have captured the essential characteristics of the groundwater flow systems in the basin. Although the observed hydraulic and temperature data are not perfectly matched by the model, it is important to note that in this study, a cross-sectional model is used to represent a three-dimensional basin-scale flow system. It is therefore not meaningful to over-fit the flow and temperature model to the field data. Rather, the aim of the study is to obtain a close enough approximation of the groundwater flow and temperature condition with which benzene transport can be simulated. Similarly, the focus of our study is on benzene transport, not on pressure generation mechanism. Therefore, the observed over-pressure in the

80−130°C). In reality, oil generation would double with every 10°C increase in temperature, thus a more realistic source term could be temperature-dependent. Moreover, the computed head profile within the upper Green River Formation above the middle marker agrees fairly well with the observed head (Fig. 9b). Finally, beneath the Green River Formation, groundwater flow in the basal Mesaverde Group is more vigorous than the Green River Formation, but less vigorous than the upper Duchesne-Uinta Formations. Within the Mesaverde Group, groundwater flows south with an average horizontal velocity of 0.01 m year^{-1}.

Fig. 10. (a) The best-fit, computed temperature (°C) in the Uinta Basin, superimposed with a conductive thermal field (dashed lines). The locations of the Altamont-Bluebell field (A-B) and Pariette Bench field (P-B) are shown. (b) The best-fit temperature anomalies (°C) in the Uinta Basin. Within the shaded region are the recharge area near the Uinta Mountains and the discharge area near the central river valley. It is to be compared with the observed anomalies shown in Fig. 3.

lower Green River Formation is represented with a constant oil generation source term to capture the overall flow behavior.

Solute transport

The groundwater flow rate and temperature computed by the best-fit flow and heat transfer model are used by the solute transport model to represent the coupled benzene migration within the oil reservoir and the basin groundwater. For each oil reservoir modeled, benzene transport by groundwater is represented by both a conservative model with no attenuation and a model with attenuation, in which case a retardation factor of 1.1 and a first-order biodegradation rate constant of 10^{-4} year^{-1} are selected. This biodegradation rate constant represents an estimated *upper* bound of the anaerobic biodegradation condition in deep basins (>1 km), approximately 2−3 orders of magnitude smaller than the anaerobic biodegradation rates estimated for shallow flow systems/soils, and approximately 2−3 orders of magnitude greater than those estimated by Head *et al.* (2003).

To simulate water washing of the Altamont-Bluebell oil reservoir, the coupled benzene transport model is first run for 5 Ma, without representing attenuation (Fig. 11a).

The simulation time is selected to allow the benzene concentration at the springs to stabilize. Simulation result of the aqueous transport model indicates that benzene dissolves into the formation water at the oil−water contact and is transported by groundwater advectively, e.g. the simulated benzene plume moves outward away from the over-pressured zone, following the groundwater flow direction. Above the oil reservoir, dissolved benzene enters the upper Green River Formation, forming a sizable geochemical plume within the central basin (maximum benzene concentration in this plume reaches up to 2 ppm). This vertically ascending plume then joins the shallow groundwater of the Duchesne-Uinta Formations and moves laterally southward until it reaches the regional groundwater discharge areas in the central river valleys. Benzene in groundwater reaches the springs in measurable concentration after 1 Ma of transport (the 0.01 ppm concentration contour shown as gray curves in Fig. 12a); after 5 Ma, benzene breakthroughs at the surface in several areas and around a quarter of the total benzene has been flushed out of the oil reservoir. The computed benzene concentration in the *co-produced* formation waters (defined as the concentration sampled near the oil−water contact in the aqueous transport model) has an average of 4.8 ppm and a range between 2.0 and 9.0 ppm, generally
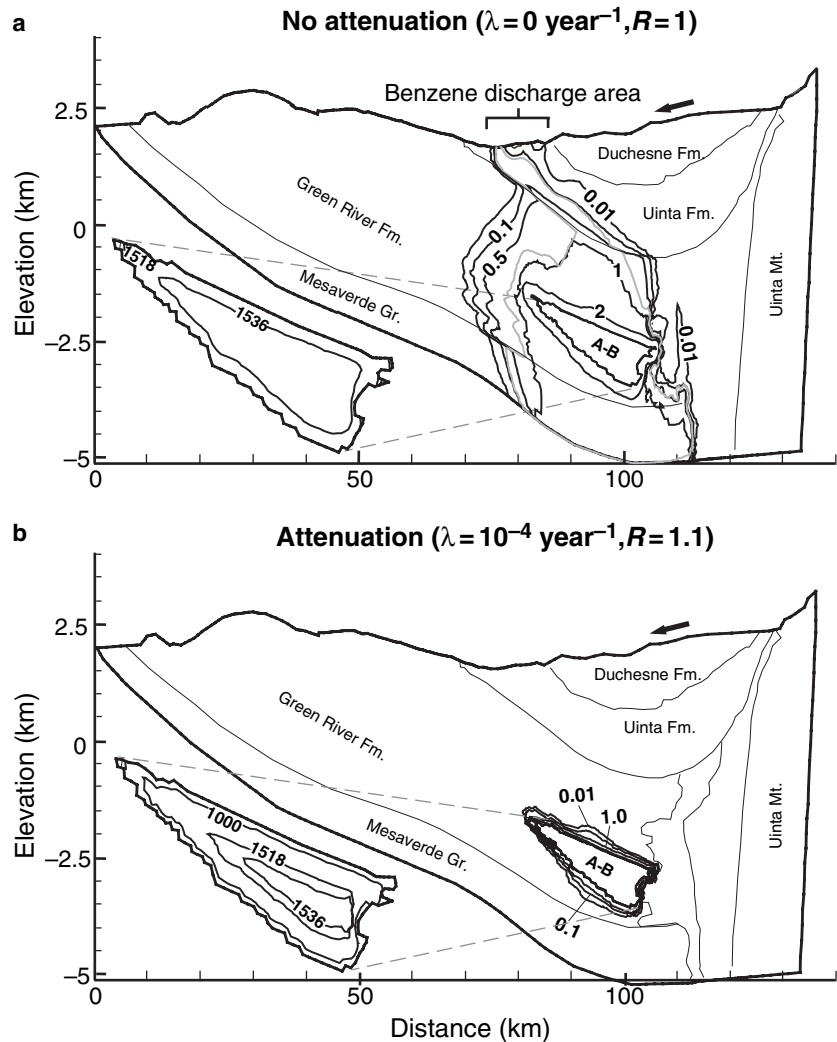
Fig. 11. (a) The computed benzene concentration (ppm) in the Uinta Basin and the Altamont-Bluebell reservoir at 5 Ma, assuming no attenuation. The grey contour is the 0.01 ppm concentration at 1 Ma. (b) The computed benzene concentration when attenuation is represented ($\lambda = 10^{-4}$ year^{-1}, R = 1.1). The arrow outside the basin indicates the general groundwater flow direction within the upper Duchesne-Uinta Formations.

matching the observed values from the Altamont-Bluebell field (average 5.6 ppm, range 3.8–9.5). In addition, a diffusional profile is simulated within the oil reservoir and no boundary layer is developed in the formation water surrounding it, quite unlike that of the sensitivity study (Zhang *et al.* in press). A possible explanation is that although benzene transport in groundwater is advection dominated, the low groundwater flow rate within the 'tight' lower Green River Formation cannot transport the dissolved benzene quickly away from the oil–water contact. Benzene diffusion within the oil reservoir may thus have kept pace with the slow mass loss at the contact caused by advection.

A second simulation is run in which benzene attenuation in groundwater is represented (Fig. 11b). At the end of 5 Ma, benzene in groundwater diminishes to below the detection limit within 4 km of the oil reservoir. Dissolved benzene is not able to reach the surface discharge areas in measurable concentration. The effect of attenuation has

also masked the advective nature of the transport, e.g. compared with the conservative model (Fig. 11a), attenuation has significantly modified the shape of the benzene plume to be ring-like, and thus similar in appearance to that of a diffusion dominated system. The computed benzene concentration in the co-produced formation waters ranges between 0.1 and 1.0 ppm, generally lower than the field measurements. This may suggest that the actual biodegradation condition at the Altamont-Bluebell field may be less vigorous than what is represented by the chosen biodegradation rate constant.

The coupled benzene transport model is also constructed for the shallower Pariette Bench oil reservoir. Both the conservative and attenuation models are run for 2 Ma (Fig. 12). Groundwater surrounding this reservoir is part of a regional topography-driven flow system, with an average upward velocity on the order of 10^{-4} m year^{-1} above the reservoir. Similar to the Altamont-Bluebell field, benzene transport in the Pariette Bench field is also dominated
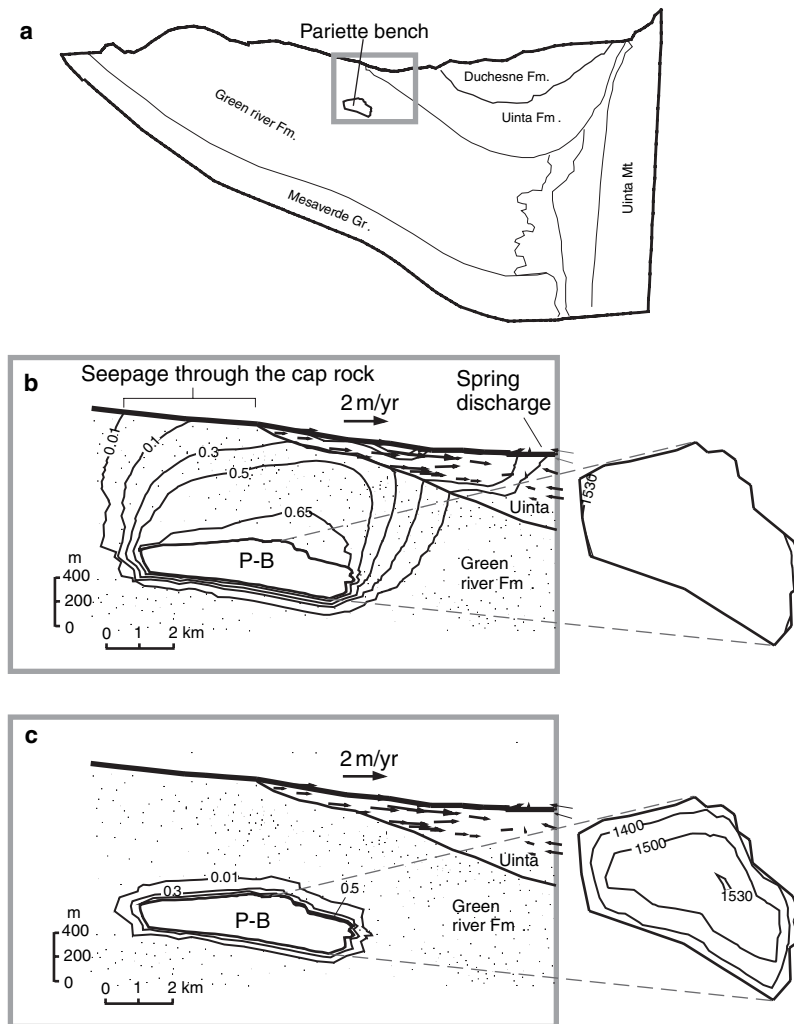
Fig. 12. (a) Location of the Pariette Bench oil reservoir in the Uinta Basin. (b) The computed benzene concentration (ppm) in the basin and the Pariette Bench reservoir at 2 Ma, without representing attenuation. The arrows indicate the direction and the magnitude of the groundwater velocity. (c) The computed benzene concentration (ppm) when attenuation is represented ($\lambda = 10^{-4}$ year^{-1}, R = 1.1).

by advection. When no attenuation is represented, the upward moving groundwater above the oil reservoir advects benzene towards the surface, forming a nearly vertical geochemical plume within the rocks of the Green River Formation (Fig. 12b). After 2 Ma of transport, benzene reaches the surface directly above the reservoir, occurring in a lateral area over 12 km. Part of the benzene enters the Uinta Formation and reaches the regional groundwater discharge areas in significant concentration (0.1–0.3 ppm). On the contrary, when attenuation is represented (Fig. 12c), benzene transport is limited to within about 1 km from the oil reservoir and the concentration of benzene at the surface does not exceed the detection limit. The attenuation model further predicts that benzene in the co-produced waters from this field has an average concentration of 0.5 ppm, while the conservative model predicts a range between 0.6 and 0.7 ppm. Both predictions do not deviate significantly from the field measurements (0.4–1.0 ppm).

DISCUSSION

Soluble benzene transport simulated for both the Altmont-Bluebell reservoir and the Pariette Bench reservoir in the Uinta Basin indicates that benzene transport by groundwater is dominated by advection. Attenuation can modify the aqueous benzene concentration (because of advection) to appear similar to a diffusion-dominated system. This has occurred because in the Uinta Basin, groundwater in contact with the oil reservoirs has relatively low velocities (on the order of 10^{-4} m year^{-1} or lower). In a more vigorous flow fields, e.g. the aquifers in the sensitivity study have a flow rate ranging from 0.005 to 2 m year^{-1} (Zhang *et al.* in press), more asymmetrical plumes can develop. The major difference between the basin represented in the sensitivity study and the Uinta Basin is that the oil reservoirs represented in the sensitivity study are in direct contact with a relatively permeable aquifer (10^{-16}–10^{-14} m^2), while the reservoirs in the Uinta Basin are encased within

the low permeability (10^{-17} m^2 or lower) rocks of the Green River Formation. Moreover, when attenuation is represented, more water washing of benzene has occurred within the oil reservoirs simulated (Figs 11 and 12). Attenuation has caused a decrease in the bulk aqueous benzene concentration near the oil-water contact, which in turn increases the gradient between the bulk aqueous concentration and the aqueous concentration at the phase boundary (which is related to the oil-phase benzene concentration via the equilibrium constant). Benzene mass flux across the oil−water contact thus increases [Equation (9a) of the sensitivity study, Zhang *et al.* in press]. Over time, this has resulted in more benzene mass loss from the oil reservoirs.

In the Altamont-Bluebell field, comparison between the observed and simulated benzene concentration in the co-produced formation waters suggests that significant biodegradation may not occur at depths in this field. The elevated temperature at this reservoir is observed to range from 80 to 130°C. It is likely that part of this field lies in a temperature range above the threshold where significant biodegradation of hydrocarbons occurs. For example, in studying the Beaufort Basin in northern Canada, Burns *et al.* (1975) noted that the subsurface temperature of 65°C seemed to mark the depth limit of biodegradation. Connan (1984) observed that biodegradation typically occurred in reservoirs cooler than 90°C. Head *et al.* (2003) suggested that biodegradation of hydrocarbons ceased at 80°C. Thus the biodegradation rate constant assigned to the transport model for the Altamont-Bluebell field may have overestimated the true conditions at depth, e.g. benzene may not be degraded until it reaches the cooler (<80°C) upper strata above the oil reservoir. The distance of benzene migration at this field could therefore be more extensive than what is predicted by the attenuation model. However, no detectable benzene is found in springs sampled at the regional groundwater discharge areas of the basin, contrary to the prediction of the conservative model. Therefore, benzene attenuation must have occurred along the flow path before reaching the surface. Similarly, in the shallower Pariette Bench field, benzene computed by the conservative model reaches the spring discharge areas in significant concentration. This is again not supported by field measurements. Benzene concentration represented in the attenuation model diminishes to below the detection limit within 1 km from the oil reservoir. Again, this distance is likely the minimum distance dissolved benzene is able to travel if the biodegradation rate chosen represents an upper limit for this field.

It is likely that several biodegradation rate constants may be required for a more accurate representation of the soluble benzene migration in the Uinta Basin, as hydrocarbon biodegradation is found to be more active in the shallower zones near the surface (Price 1985). For example, benzene anaerobic biodegradation rate constant estimated for shallow flow systems is 4−5 orders of magnitude higher than that estimated for deeper oil fields. Moreover, anaerobic biodegradation of hydrocarbons proceeds much more slowly than aerobic biodegradation (Milner *et al.* 1977). The boundary between these two biodegradation regimes could be delineated by the depth at which significant oxygen is dissolved in groundwater (Milner *et al.* 1977). The thickness of this 'aeration zone' varies, but it can reach up to a depth of 600 m within regional aquifers (Andreev *et al.* 1968). Both types of microorganisms could be introduced into the deep subsurface by meteoric recharge into a basin (Bailey *et al.* 1973; Tseng *et al.* 1998), while recent studies also suggest that it is likely these microbes could have existed when the sediments were first laid down (Head *et al.* 2003). It should be further pointed out that dissolved oxygen in groundwater can react with hydrocarbons inorganically (Andreev *et al.* 1968). Sulfur formed through thermal cracking of kerogen can also destroy light hydrocarbons in the deep, hot depths of sedimentary basins (Hunt 1975). It can be speculated that in the Altamont-Bluebell field where oil is actively being generated, abiogenic reactions involving sulfur may also play a role in attenuating benzene. However, the extent and rate of these chemical reactions in the Uinta Basin are currently not known.

CONCLUSIONS

In this study, numerical modeling and field sampling are conducted to gain an insight into the transport and attenuation of the petroleum-derived benzene in the Uinta Basin. Oils and formation waters were sampled at the Altamont-Bluebell and Pariette Bench oil fields. Springs located down gradient from the oil fields were also sampled. Benzene was found in significant concentration in oils (up to 19 000 ppm), moderate concentration in oil-field waters (up to 17.7 ppm), but below the detection limit in springs. A suite of mathematical models is constructed to represent the groundwater flow and heat transfer in the basin and the coupled benzene transport in groundwater and oil reservoir. The groundwater flow and heat transfer model is first calibrated using available pressure and temperature data across the basin. The observed excess head within the lower Green River Formation is approximately reproduced as well as the observed convective temperature anomalies within the upper Duchesne-Uinta Formations. Using the best-fit computed flow and temperature, coupled benzene transport is simulated for 2−5 Ma for the Pariette Bench and the Altamont-Bluebell oil reservoirs, respectively. Results indicate that soluble benzene transport in the Uinta Basin is dominated by groundwater advection. Attenuation rapidly diminishes benzene concentration in the formation groundwater to below the detection limit.

For the given upper limit of the biodegradation rate, the minimum transport distance is 1 and 4 km for the Pariette Bench reservoir and the Altamont-Bluebell reservoir, respectively. Attenuation also controls the amount of water washing within the oil reservoir over time. In general, models that represent benzene attenuation produce results more consistent with field observations.

REFERENCES

Andreev PF, Bogomolov AI, Dobryanskii AF, Kartsev AA (1968) *Transformation of Petroleum in Nature.* Pergamon, Oxford.

Bailey NJL, Krouse HR, Evans CR, Rogers MA (1973) Alteration of crude oil by waters and bacteria − evidence from geochemical and isotropic studies. *AAPG Bulletin*, **57**, 1276−90.

Bredehoeft JD, Wesley JB, Fouch TD (1994) Simulations of the origin of fluid pressure, fracture generation, and the movement of fluids in the Uinta Basin. *AAPG Bulletin*, **78**, 1729−47.

Burns BJ, Hogarth JTC, Milner CWD (1975) Properties of Beaufort Basin liquid hydrocarbons. *Bulletin of Canadian Petroleum Geology*, **23**, 295−303.

cBurtell SG, Jones VT (1996) Benzene content of subsurface brines can indicate proximity of oil, gas. *Oil and Gas Journal*, **3**, 59−63.

Chapman DS, Keho TH, Bauer MS, Picard MD (1983) Heat flow in the Uinta Basin determined from bottom hole temperature (BHT) data. *Geophysics*, **49**, 453−66.

Chidsey TC, Laine MD (1992) The Fractured Green River and Wasatch Formation of the Uinta Basin, Utah: targets for horizontal drilling, In: *Hydrocarbon and Mineral Resources of the Uinta Basin, Utah and Colorado*, pp. 123−34. Utah Geological Association Guidebook, 20, Salt Lake City, UT.

Connan J (1984) Biodegradation of crude oils in reservoirs. *Advances in Petroleum Geochemistry*, **1**, 299−335.

Fouch TD (1975) Lithofacies and related hydrocarbon accumulations in Tertiary strata of the western and central Uinta Basin. In: *Symposium on Deep Drilling Frontiers in the Central Rocky Mountains*, (ed Bolyard DW). Rocky Mountain Association of Geologists Special Publication, pp. 163−73.

Fouch TD (1981) Distribution of rock types, lithologic groups, and interpreted depositional environments for some lower Tertiary and upper Creatcious rocks from outcrops at Willow Creek Indian Canyon through the subsurface of Duchesne and Altamont oil fields, southwest to north-central parts of the Uinta Basin, Utah. *Oil and Gas Investigations Chart*, 2 Sheets, USGS, Reston, VA.

Fouch TD, Nuccio VF, Osmond JC, McMillan L, Cashion WB, Wandrey CJ (1992a) Oil and Gas in uppermost Cretaceous and Tertiary Rock, Uinta Basin, Utah. In: *Hydrocarbon and Mineral Resources of the Uinta Basin, Utah and Colorado, Utah Geological Association Guidebook 20*, (eds Fouch TD, Nuccio VF, Chidsey TC), Utah Geological Association, pp. 9−47, Salt Lake City, UT.

Fouch TD, Wandrey CJ, Pitman JK, Nuccio VF, Schmoker JW, Rice DD, Johnson RC, Dolton GL (1992b) Natural gas accumulations in low permeability Tertiary and Cretaceous (Campanian and Maastrichtian) rock, Uinta basin, Utah. U.S. Department of Energy, Office of Fossil Energy, DOE/MC/20422-3051 (DEC92001132).

Freeze RA, Cherry JA (1979) *Groundwater.* Prentice-Hall, Englewood Cliffs.

Garven G (1989) A hydrogeologic model for the formation of the giant oil sands deposits of the Western Canada sedimentary basin. *American Journal of Science*, **289**, 105−66.

Gelhar L (1993) *Stochastic Subsurface Hydrology.* Prentice Hall, Englewood Cliffs, New Jersey.

Ground Water Atlas of the United States (1995) *Segment 2, Hydrologic Investigations Atlas 730-C.* USGS, Reston, VA.

Head IM, Jones DM, Larter SR (2003) Biological activity in the deep subsurface and the origin of heavy oil. *Nature*, **426**, 344−52.

Hester TC, Schmoker JW (1993) Porosity, Depth, and Thermal−Maturity Data for Sandstones of the Anadarko Basin, Oklahoma, and Other Selected Locations in the Northern Hemisphere. USGS Open-File Report, 93−230.

Hunt JM (1975) Is there a geochemical depth limit for hydrocarbons. *Petroleum Engineering*, **46**, 112−24.

Keighin CW, Sampath K (1982) Evaluation of pore geometry of some low-permeability sandstones-Uinta Basin. *Journal of Petroleum*, **34**, 1, 65−70.

Lucas PT, Drexler JM (1975) Altamont-Bluebell: a major fractured and over-pressured stratigraphic trap, Uinta Basin, Utah. In: *Rocky Mountain Association of Geologists Symposium*, 265−73.

Mailloux BJ, Person M, Kelley S, Dunbar N, Cather S, Strayer S, Hudleston S (1999) Tectonic controls on the hydrogeology of the Rio Grande Rift, New Mexico. *Water Resources Research*, **35**, 2641−59.

McCoy RM, Young SA (1992) Sage brush associated with lineaments shows influence of hydrocarbon microseepage in high production areas of the Altamont-Bluebell oil field. In: *Hydrocarbon and Mineral Resources of the Uinta Basin, Utah and Colorado.* Utah Geological Association Guidebook, **20**, 135−42.

McPherson BJOL, Bredehoeft JD (2001) Overpressures in the Uinta Basin, Utah: Analysis using a three-dimensional basin evolution model. *Water Resources Research*, **37**, 857−71.

McPherson BJOL, Jarrard RD, Bredehoeft JD (2000) *Controls on Intergranular Porosity and Permeability in the Northern Uinta Basin, Utah.* Report for USGS, purchased from USGS, Branch of Information Services, Denver Federal Center, Denver, CO.

Milner CWD, Rogers MA, Evans CR (1977) Petroleum transformations in reservoirs. *Journal of Geochemical Exploration*, **7**, 101−53.

Narr W, Currie JB (1982) Origin of fracture porosity−example from Altamont field, Utah. *AAPG Bulletin*, **66**, 1231−47.

Pitman JK, Fouch TD, Goldhaber MB (1982) Depositional setting and diagenetic evolution of some Tertiary unconventional reservoir rocks, Uinta basin, Utah. *AAPG Bulletin*, **66**, 1581−96.

Price LC (1985) A critical overview of and proposed working model for hydrocarbon microseepage. *USGS Open-File Report*, 85−271.

Robson SG, Banta (1995) Ground Water Atlas of the United States, Segment 2 − Arizona, Colorado, New Mexico, and Utah. *USGS Investigations Atlas 730-C*, 32p., USGS, Reston, Virginia. (http://capp.water.usgs.gov/gwa/).

Ruble TE, Philp RP (1998) Stratigraphy, depositional environments and organic geochemistry of source-rocks in the Green River petroleum system, Uinta Basin, Utah, in Modern and ancient lake systems. *Utah Geological Association Guidebook*, **26**, 289−321.

Ruble TE, Lewan MD, Philp RP (2001) New insights on the Green River petroleum system in the Uinta basin from hydrous pyrolysis experiments. *AAPG Bulletin*, **85**, 1333−71.

Schmoker JW, Nuccio VF, Pitman JK (1992) Porosity Trends in Predominantly Nonmarine Sandstones of the Upper Cretaceous Mesaverde Group, Uinta and Piceance Basins, Utah and Colorado, in Hydrocarbon and Mineral Resources of the Uinta Basin, Utah and Colorado. *Utah Geological Association Guidebook*, **20**, 111−22.

Spencer CW (1987) Hydrocarbon Generation as a Mechanism for Overpressuring in Rocky Mountain Region. *AAPG Bulletin*, **71**, 368−88.

Sweeney JJ, Burnham AK, Bruan RL (1987) A model of hydrocarbon generation from type I Kerogen: Application to Uinta Basin. *AAPG Bulletin*, **71**, 967−85.

Tóth J (1963) A theoretical analysis of groundwater flow in small drainage basins. *Journal of Geophysical Research*, **68**, 4795−812.

Tseng H, Person MA, Onstott TC (1998) Hydrogeologic constraint on the origin of deep subsurface microorganisms within a Triassic Basin. *Water Recourses Research*, **34**, 937−48.

Utah State Water Plan − Uintah Basin (1999) Utah Board of Water Resources, prepared by the Division of Water Resources of the State Water Plan Steering Committee, http://www.water.utah.gov/planning/swp/unitah/.

Weisenberg DA, Bodennec G, Brooks JM (1981) Volatile liquid hydrocarbons around a productive platform in the northwest Gulf of Mexico. *Bulletin Environmental Contamination Toxicology*, **27**, 167−74.

Willett SD, Chapman DS (1987) On the use of thermal data to resolve and delineate hydrologic flow systems in sedimentary basins: an example from the Uinta Basin, Utah. In: *Proceedings of the Third Annual Canandian/American Conference on Hydrogeology; Hydrology of Sedimentary Basins − Applications to Exploration and Exploitation*, pp. 159−68. National Water Well Association, Dublin, OH.

Willett SD, Chapman DS (1989) Temperatures, fluid Flow and heat Transfer mechanisms in the Uinta Basin. *Geophysical Monograph*, **47**, IUGG Volume 2, 29−33.

Young SA, McCoy RM (1990) Association among Landsat TM data, hydrocarbon microseepage and geobotanical anomalies in the Uinta Basin, Utah. In: *10 Annual International Geoscience and Remote Sensing Symposium*, pp. 975−78. Institute of Electrical and Electronics Engineers, New York.

Zarrella WM, Mousseau RJ, Coggeshall ND, Norris MS, Schrayer GJ (1967) Analysis and significance of hydrocarbons in subsurface brines. *Geochimica et Cosmochimica Acta*, **31**, 1155−66.

Zhang Y, Person MA, Merino E (2005) Hydrologic and geochemical controls on soluble benzene migration in sedimentary basins. *Geofluids*, **5**, 83−105.

NOMENCLATURE

∇	Gradient operator
$\cdot$	Inner product
h	Hydraulic head
$\vec{q}$	Darcy flux vector: $\vec{q} = \begin{bmatrix} q_x \\ q_z \end{bmatrix}$
ρ_f	Density of water
ρ_{oil}	Density of oil
ρ_r	Relative water density, $\rho_r = (\rho_f - \rho_0)/\rho_0$
μ_r	Relative water viscosity $\mu_r = \mu_0/\mu_f$
$\mathbf{K}$	Hydraulic conductivity tensor: $\mathbf{K} = \begin{bmatrix} K_{xx} & K_{xz} \\ K_{zx} & K_{zz} \end{bmatrix}$
q'	Oil generation source term
τ	Relaxation time for over-pressure due to sediment loading
L	Thickness of low-permeability deposits
S_s	Storage of low-permeability deposits
K	Hydraulic conductivity of low-permeability deposits
C_{aq}	Measured benzene concentration in oil-field waters
C_{oil}	Measured benzene concentration in oils